

Differentiating inflamed and normal lungs by the apparent reaction rate constants of lactate dehydrogenase probed by hyperpolarized ^{13}C labeled pyruvate

He N. Xu^{1,2}, Stephen Kadlecek¹, Hooria Shaghghi¹, Huaqing Zhao³, Harilla Profka¹, Mehrdad Pourfathi¹, Rahim Rizzi¹, Lin Z. Li^{1,2}

¹Department of Radiology, ²Britton Chance Laboratory of Redox Imaging, Johnson Research Foundation, Perelman School of Medicine, University of Pennsylvania, Philadelphia, PA 19104, USA; ³Department of Clinical Sciences, Temple University School of Medicine, Philadelphia, PA 19140, USA

Correspondence to: Lin Z. Li, PhD. Department of Radiology, Perelman School of Medicine, University of Pennsylvania, Philadelphia, PA 19104, USA. Email: linli@mail.med.upenn.edu.

Background: Clinically translatable hyperpolarized (HP) ^{13}C -NMR can probe *in vivo* enzymatic reactions, e.g., lactate dehydrogenase (LDH)-catalyzed reaction by injecting HP ^{13}C -pyruvate into the subject, which is converted to ^{13}C labeled lactate by the enzyme. Parameters such as ^{13}C -lactate signals and lactate-to-pyruvate signal ratio are commonly used for analyzing the HP ^{13}C -NMR data. However, the biochemical/biological meaning of these parameters remains either unclear or dependent on experimental settings. It is preferable to quantify the reaction rate constants with a clearer physical meaning. Here we report the extraction of the kinetic parameters of the LDH reaction from HP ^{13}C -NMR data and investigate if they can be potential predictors of lung inflammation.

Methods: Male Sprague-Dawley rats (12 controls, 14 treated) were used. One dose of bleomycin (2.5 U/kg) was administered intratracheally to the treatment group. The lungs were removed, perfused, and observed by the HP-NMR technique, where a HyperSense dynamic nuclear polarization system was used to generate the HP ^{13}C -pyruvate for injecting into the lungs. A 20 mm $^1\text{H}/^{13}\text{C}$ dual-tuned coil in a 9.4-T Varian vertical bore NMR spectrometer was employed to acquire the ^{13}C spectral data every 1 s over a time period of 300 s using a non-selective, 15-degree radiofrequency pulse. The apparent rate constants of the LDH reaction and their ratio were quantified by applying ratiometric fitting analysis to the time series data of ^{13}C labeled pyruvate and lactate.

Results: The apparent forward rate constant $k_p=(3.67\pm 3.31)\times 10^{-4}\text{ s}^{-1}$, reverse rate constant $k_r=(4.95\pm 2.90)\times 10^{-2}\text{ s}^{-1}$, rate constant ratio $k_p/k_r=(7.53\pm 5.75)\times 10^{-3}$ for the control lungs; $k_p=(11.71\pm 4.35)\times 10^{-4}\text{ s}^{-1}$, $k_r=(9.89\pm 3.89)\times 10^{-2}\text{ s}^{-1}$, and $k_p/k_r=(12.39\pm 4.18)\times 10^{-3}$ for the inflamed lungs at the 7th day post treatment. Wilcoxon rank-sum test showed that the medians of these kinetic parameters of the 7-day cohort were significantly larger than those of the control cohort ($P<0.001$, $P=0.001$, and $P=0.019$, respectively). The rate constants of individual lungs correlated significantly with the histology scores of neutrophils and organizing pneumonia foci but not macrophages. Both k_p and k_p/k_r positively correlated with lactate labeling signals. No correlation was found between k_r and lactate labeling signals.

Conclusions: The results indicate bleomycin-induced lung inflammation significantly increased both the forward and reverse reaction rate constants of LDH and their ratio at day-7 after bleomycin treatment.

Keywords: Hyperpolarization; NMR spectroscopy; lactate dehydrogenase (LDH) reaction; ^{13}C -pyruvate and lactate; lung inflammation

Submitted Jan 10, 2016. Accepted for publication Feb 01, 2016.

doi: 10.3978/j.issn.2223-4292.2016.02.04

View this article at: <http://dx.doi.org/10.3978/j.issn.2223-4292.2016.02.04>

Introduction

Lung injuries including pulmonary inflammation and fibrosis can be induced by radiation therapy and toxic agents such as the anti-tumor drug bleomycin (1-3). This predicament demands *in vivo* non-invasive methods for assessing lung injury in the early stage and stabilizing, treating or even reversing the condition. Although ^1H -MRI methods and MRI using hyperpolarized (HP) inert gas inhalation have been used to non-invasively characterize lung injuries, they do not allow direct exploration of cellular metabolism, which may indicate metabolic abnormality of lung tissue prior to irreversible functional and structural changes.

On the other hand, HP ^{13}C -NMR has been increasingly investigated for its ability to image metabolism as a potential biomarker for cancer detection and treatment response (4-12) and lung injury (13-16). The signals from HP ^{13}C species allow one to probe the relevant enzymatic reactions *in vivo*. For instance, detecting tissue inflammation using HP ^{13}C -pyruvate has shown that inflammation caused an increase in lactate labeling via the reaction catalyzed by lactate dehydrogenase (LDH) (17,18). Previously, we reported the results from HP $[1-^{13}\text{C}]$ pyruvate studies of bleomycin-induced lung injury (19). We showed that the bleomycin-treated lungs on the 7th day post-treatment had significantly higher lactate labeling than the control lungs.

However, the lactate labeling signals (e.g., peak intensity or signals integrated over the time course) observed in HP ^{13}C -NMR experiments are dependent on instrument settings, such as degree of polarization achieved and radio-frequency pulse power used, and biological factors such as the rate of perfusion. Although the lactate-to-pyruvate ratios (such as the ratios of their peak or integrated signals) may mitigate the influences of these factors, the exact biochemical/biological bases for the validity of metabolite labeling signals or their ratios are unclear. In principle, a more reliable approach is to determine the apparent rate constants of the LDH reaction, which have a clearer biochemical/biological meaning. In this paper, we take the ratiometric analysis approach (20,21) to analyze the lung data [reference (19) plus new data from 6 additional lungs] in order to generate new parameters and insight into lung injury. Specifically, we report the quantification of both forward and backward apparent rate constants and their ratio of LDH-catalyzed reaction to discriminate between inflamed and normal lungs and correlate them with histological measurements. A preliminary report of this analysis was published in a conference proceeding (22).

Materials and methods

Lung inflammatory model preparation and MRS

The details on experimental preparation and NMR spectroscopy can be found in the previous publication (19). Briefly, as shown in the study scheme (*Figure 1*), male Sprague-Dawley rats (250–300 g) of eight weeks old were randomly divided into the control (N=12) and the treatment group (N=14). The anesthetized rats were given bleomycin one time at a concentration of 2.5 U/kg through intratracheal instillation to induce lung injuries which were confirmed by the semi-quantitative histological scores based on the signs of inflammation. The treated rats were maintained under similar environments and dietary conditions to the control rats. Rat lungs at the 7th day (7-day group, N=11) and the 21st day (21-day group, N=3) post-induction were removed after thoracotomy. All lungs were perfused with 400 mL modified Krebs-Henseleit buffer (T=36.5±1 °C and pH=7.4±0.1) and oxygenated under a constant flow of 95:5 O₂/CO₂ at 1 atm.

The HP- ^{13}C -NMR spectra of the perfused lungs were obtained using a HyperSense dynamic nuclear polarization system (Oxford Instruments) and a 20 mm $^1\text{H}/^{13}\text{C}$ dual-tuned coil in a 9.4-T Varian vertical bore NMR spectrometer. A 10 mL of 32 mM HP $[1-^{13}\text{C}]$ pyruvate was infused through the pulmonary artery at 10 mL/min. The signals of $[1-^{13}\text{C}]$ pyruvate and its metabolites (e.g., $[1-^{13}\text{C}]$ lactate) were collected every 1 s over a time period of 300 s using a non-selective, 15-degree radiofrequency pulse. The maximum SNR [maximum pyruvate signal/standard deviation (SD) of the baseline] was at least several hundred in each experiment. All perfused lungs were observed by ^{31}P -NMR spectroscopy to confirm normal ATP metabolism (ATP/Pi>1) and lung viability before and after HP-NMR observation.

H&E staining

After NMR studies, three perfused lungs from each group were H&E-stained to confirm the lung injuries (23). Five tissue sections were stained for each lung. The levels of neutrophils (N), macrophages (M), organizing pneumonia foci (O), and lymphocytes (L) were scored with a grade 0–4 blindly by a pulmonary pathologist as detailed in our previous publication (19). Briefly, for each cell type, grade 0 was assigned to lungs with minimal cell density and grade 4 was assigned to lungs with severe and widely distributed inflammatory cells. Ratings were averaged across five sections of each lung and the mean scores were then assigned to the

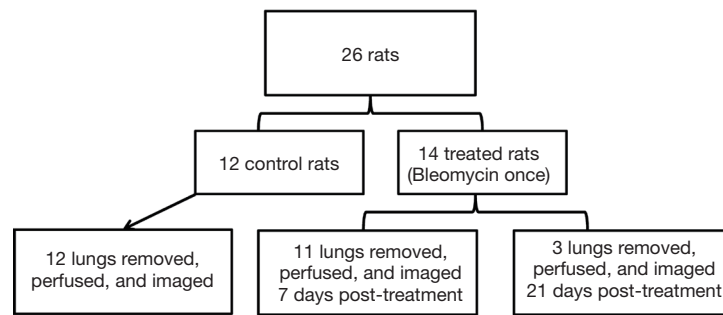


Figure 1 The scheme of the study.

lung for each cell type. These scores were further analyzed for statistical significance with the linear mixed-effect model where tissue section was taken as the repeated measure.

Extraction of the kinetic parameters

The signals of pyruvate and lactate at each time point were obtained by least-squares fitting of ¹³C spectra and were normalized to the total pyruvate signal integrated over the period of signal acquisition (300 s) as described previously (19). The time courses of these signals were further analyzed using the ratiometric fitting method (20) with the assistance of customized Matlab routines to obtain the apparent rate constants of the pseudo first order LDH-catalyzed reaction. The basic concept of the ratiometric fitting method is summarized below.

Assuming both HP ¹³C labeled pyruvate and lactate have the same relaxation time T₁ (ρ=1/T₁), and solving for P(t) and L(t) from the two-site exchange model, we have the following formula as presented in our previous work (20):

$$P(t) = P(0)(k_i e^{-\rho t} + k_p e^{-(\rho+k_i+k_p)t}) / (k_i + k_p) + L(0)(k_i e^{-\rho t} - k_i e^{-(\rho+k_i+k_p)t}) / (k_i + k_p) \quad [1a]$$

$$L(t) = P(0)(k_p e^{-\rho t} - k_p e^{-(\rho+k_i+k_p)t}) / (k_i + k_p) + L(0)(k_p e^{-\rho t} + k_i e^{-(\rho+k_i+k_p)t}) / (k_i + k_p) \quad [1b]$$

where L(0) and P(0) are the peak intensities at t=0, k_p and k_i are the apparent 1st order forward and reverse rate constant for the conversion of pyruvate to lactate and lactate to pyruvate, respectively. By dividing Eq. 1b by Eq. 1a we have

$$R(t) = \frac{r[1 + R(0)] + [R(0) - r]e^{-st}}{1 + R(0) + [r - R(0)]e^{-st}} \quad [2]$$

where R(t) = L(t)/P(t), r = k_p/k_i, and s = k_p + k_i. By fitting Eq. 2 to the ratio time course R(t) with r and s as independent variables, we obtain k_p and k_i.

In practice, the ratiometric analysis model fit to the time course of the ratio signal of lactate to pyruvate was applied for a limited time window. The time window consideration was based on the SNR ≥3, where the initial time point corresponded to the first appearance of significant lactate signal and the end point corresponded to the end of the pyruvate injection (20). Data with SNR <3 were rejected, eliminating the late-time measurements that were imprecise due to T₁ relaxation and signal decay. Approximately, 20–50 out of 300 data points were included for each fitting.

Statistical analysis

The apparent forward (k_p) and reverse (k_i) rate constants and their ratio (k_p/k_i) were averaged across the samples for each group. Wilcoxon rank-sum test and linear-mixed effect model were used respectively to detect the statistical significance for the kinetic differences and histological differences between the control and the treated group. Significant correlations between various variables were identified with linear regression. For all statistical tests, P<0.05 was taken as significant. All statistical tests were performed with IBM’s SPSS (version 20).

Results

Kinetic parameters

Figure 2A,B shows typical stacked plots of the HP ¹³C-NMR spectra at a series of time points for an inflamed and a normal lung, respectively. For easier comparison, one-dimensional graphs of the summed HP ¹³C-NMR spectra with the same scaling factors were also inserted. The lactate peak (red) was approximately 3 times larger in the inflamed lung.

The time series data of the typical HP ¹³C-pyruvate and lactate signals and their ratios are shown in Figure 2C-F,

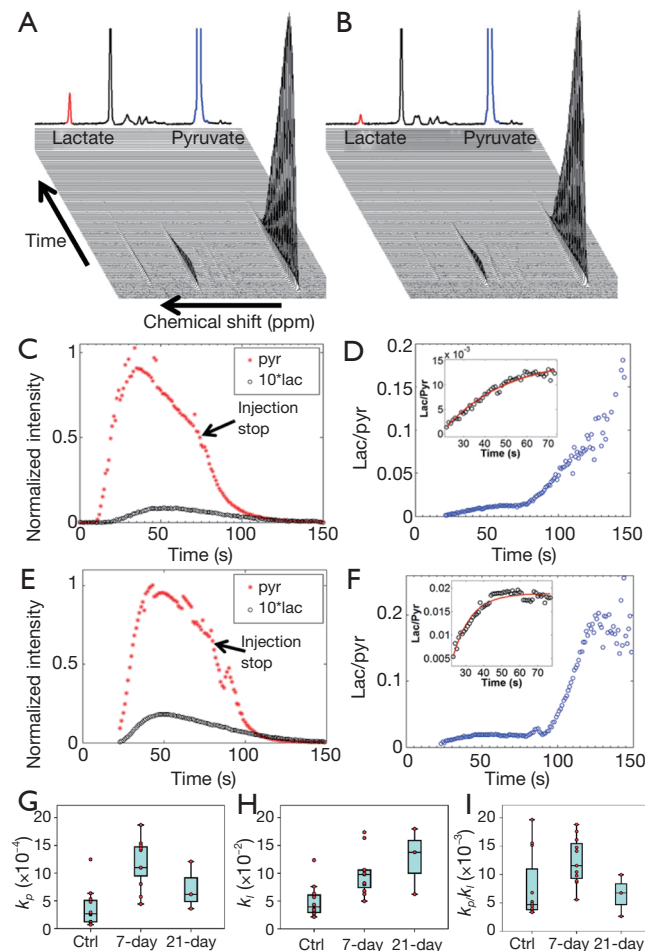


Figure 2 HP- ^{13}C -NMR of lungs: typical spectra, data analysis and results. (A,B) Typical stacked plots of the HP- ^{13}C -NMR spectra showing major metabolites involved in the LDH-catalyzed reaction of the rat lungs (A, inflamed; B, normal). The x-axis represents chemical shift (ppm) and the y-axis represents time course. (C–F) Typical time courses of ^{13}C -pyr, ^{13}C -lac (multiplied by a factor of 10) and their ratios (^{13}C -lac/ ^{13}C -pyr). C and D represent a normal lung; (E,F) represent a 7-day post-treatment lung; the inserts in (D,F) are the ratiometric fittings of the ratio time courses. (G–I) Graphical description of the results from all lungs using the dotted boxplots of the rate constants k_p , k_i , and their ratio, respectively, showing the minimum, first quartile (Q1), median, third quartile (Q3), and maximum (see Table 1).

where Figure 2C,D represents the control group data and Figure 2E,F the 7-day group. It is evident that bleomycin treatment was associated with higher lactate signals. The time courses of lactate/pyruvate ratios exhibited an initial period of steady increase and gradually plateaued until the end of agent

injection. The ratiometric analysis model (Eq. 2) fit well to these segments (see inserts in Figure 2D,F), producing the reaction rate constants.

The ratiometric fitting results for the control, the 7-day and 21-day post-treatment groups are tabulated in Table 2 showing the mean values \pm SDs for the rate constants k_p and k_i and the rate constant ratio k_p/k_i . Compared to the control group, the treatment groups appeared to have increased mean rate constants and rate constant ratios except for the mean rate constant ratio of the 21-day treatment group. Since these rate constants did not have normal distributions, Wilcoxon rank-sum test (instead of Student's *t*-test) was performed for statistically comparing the control and the 7-day group (Table 1). Although the 21-day group appeared to have higher mean values of k_p and k_i than the control, we did not perform the Wilcoxon rank-sum test to compare this group with the others due to the small sample size ($N=3$). The boxplots (Figure 2G–I) give a straightforward view of the comparison between the control and the treatment groups while also showing the distribution of individual lungs. We can see that the medians of both the forward rate constant k_p and reverse rate constant k_i of the 7-day group were larger than that of the control group ($P<0.001$ and $P=0.001$, respectively). The median rate constant ratio k_p/k_i was also higher in the 7-day group ($P=0.019$).

Correlations between the kinetic parameters and histology scores

As shown in Figure 3A, the histologically determined levels of neutrophils (N), macrophages (M), organizing pneumonia foci (O), and lymphocytes (L) were all significantly higher in the treated groups and the 7-day group had more O but less M than those for the 21-day group. High neutrophil level indicates acute stress (such as inflammation) and high macrophage level indicates more cell death. Organizing pneumonia foci are histologic patterns of alveolar inflammation. When we pooled the three groups (control, 7-day and 21-day) and correlated the kinetic parameters with the average histology scores for individual lungs, we found that both k_p and k_i had a significantly positive linear correlation with the levels of neutrophil and k_p also positively correlated with organizing pneumonia foci levels (Figure 3B,C). No significant correlation was found when correlating the kinetic parameters with macrophages or lymphocytes. Note that the results shown in Figure 3 should be interpreted with caution, since we only had three lungs from each group for

Table 1 Wilcoxon rank-sum test results on the kinetic parameters

| Parameters | Control (N=12) | | | Treated group (7-day) (N=11) | | | P value* |
|---------------------------------------|----------------|------|------|------------------------------|------|-------|----------|
| | Median | Q1 | Q3 | Median | Q1 | Q3 | |
| $k_p (\times 10^{-4} \text{ s}^{-1})$ | 2.70 | 1.22 | 5.21 | 11.00 | 8.04 | 14.99 | <0.001 |
| $k_i (\times 10^{-2} \text{ s}^{-1})$ | 3.94 | 2.84 | 6.21 | 9.78 | 6.82 | 10.61 | 0.001 |
| $k_p/k_i (\times 10^{-3})$ | 4.69 | 3.69 | 13.1 | 11.54 | 8.85 | 16.10 | 0.019 |

*, exact test P value.

Table 2 The apparent rate constants of the LDH reaction and their ratios (mean \pm SD)

| Groups | $k_p (\times 10^{-4} \text{ s}^{-1})$ | $k_i (\times 10^{-2} \text{ s}^{-1})$ | $k_p/k_i (\times 10^{-3})^*$ |
|----------------------------|---------------------------------------|---------------------------------------|------------------------------|
| Control (N=12) | 3.67 \pm 3.31 | 4.95 \pm 2.90 | 7.53 \pm 5.75 |
| Inflammation (7-day, N=11) | 11.71 \pm 4.35 | 9.89 \pm 3.89 | 12.39 \pm 4.18 |
| Inflammation (21-day, N=3) | 6.81 \pm 4.61 | 12.12 \pm 6.93 | 6.68 \pm 4.02 |

*, k_p/k_i for each individual lung was first obtained from the fitting followed by averaging them across the group.

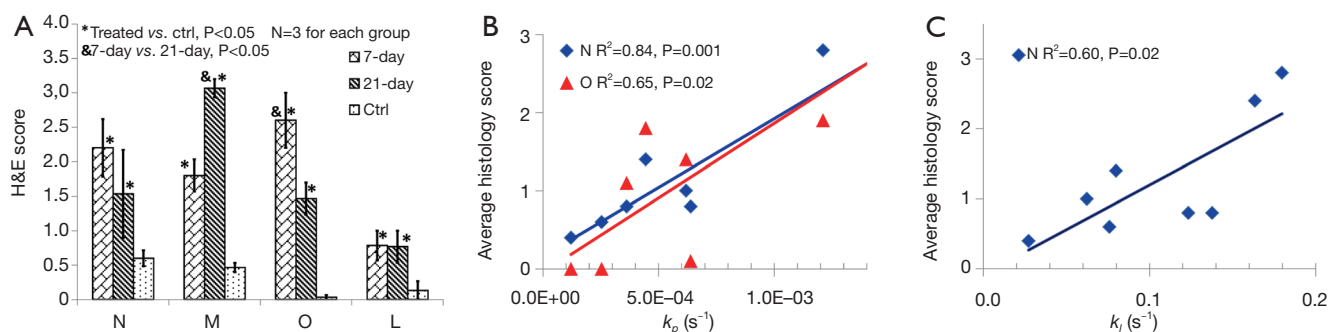


Figure 3 Histological scores of the lungs and their correlations with the rate constants. (A) The treated groups had significantly higher levels of neutrophils (N), macrophages (M), organizing pneumonia foci (O), and lymphocytes (L) compared to the control group; from 7- to 21-day, more macrophages appeared but organizing pneumonia foci became less; (B) the rate constant k_p was positively correlated with the N and O levels; (C) the rate constant k_i was positively correlated with the N levels. The P value indicates the statistical significance of the linear correlation of the data and R^2 indicates the square of the correlation coefficient.

H&E staining and scoring.

Correlations between the kinetic parameters and lactate intensities

Figure 4 shows the positive correlation of both k_p and k_p/k_i to the maximum lactate signals of individual lungs for both the control and 7-day groups. Similarly, we also found that both k_p and k_p/k_i positively correlated with the lactate signals integrated over the same time segment of the ratiometric analysis (data not shown). We did not identify any correlation between k_i and the various lactate signals for

either group.

Discussion

By using the ratiometric data analysis method we previously developed (20,21), we quantified the kinetic parameters of the LDH-catalyzed inter-conversion between pyruvate and lactate. Kinetic modeling of the HP-NMR data using the two-site exchange model has been one of the key components for interpreting the data (24). The conventional method is to directly fit the differential equations (DE) of the two-site exchange model to the time courses of

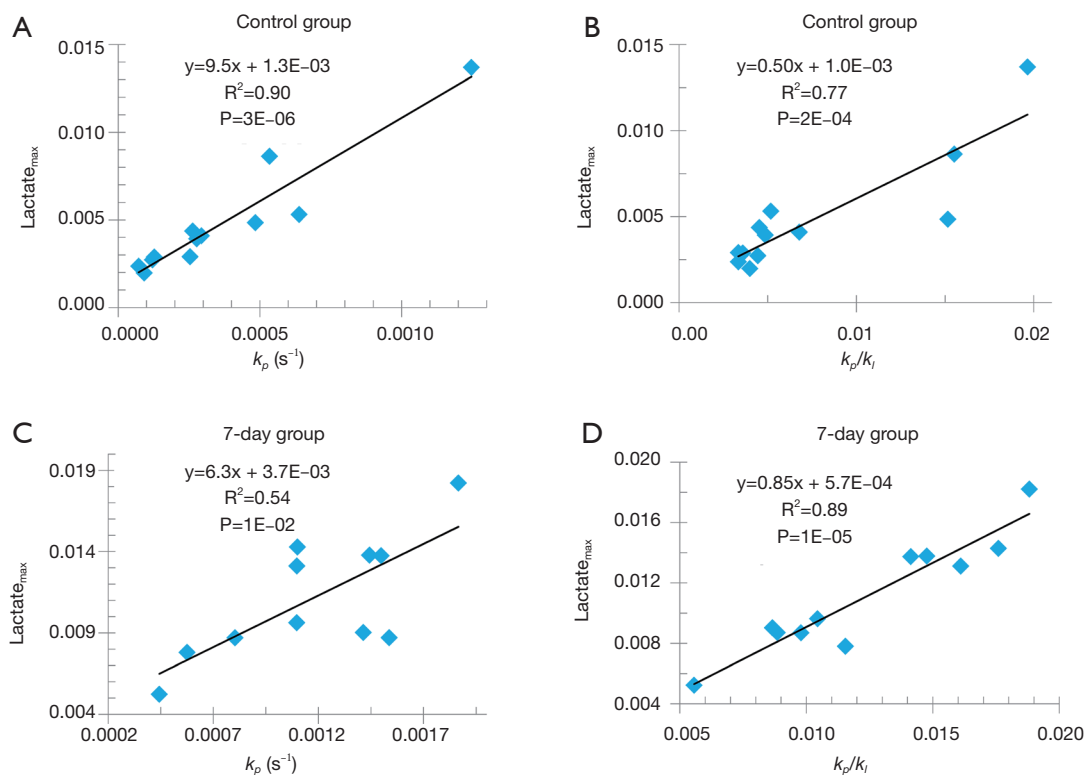


Figure 4 Linear correlations between the kinetic parameters (k_p and k_p/k_i) and maximum lactate signals. (A,B) Control group; (C,D) group of 7-day post-treatment. The P value indicates the statistical significance of the linear correlation of the data and R^2 indicates the square of the correlation coefficient.

the signals of the metabolites and extract the kinetic information from the fitting parameters. However, our previous work showed that the LDH enzymatic kinetics observed by HP-NMR is in near-equilibrium and satisfies the two-site exchange model only for a specific time window (20). We also reported our development of the ratiometric fitting method which fits the two-site exchange model to the time course of the ratio $R(t)$ [$R(t) = L(t)/P(t)$] for obtaining the apparent forward rate constant k_p and the reverse rate constant k_i as well as their ratio k_p/k_i . Compared with the conventional fitting methods to extract rate constants, this ratiometric approach has several advantages (20). Firstly, it only uses two fitting parameters, less than the conventional fitting methods. Secondly, it is expected to be less sensitive to instrument settings or experiment protocols such as the radio frequency flip angle and degree of polarization because these factors are cancelled out in principle by taking signal ratios. Thirdly, it constrains the reverse rate constant with less relative error than the DE method. These advantages combine such that the ratio fitting method can detect significant differences in the

forward rate constant between an indolent and a metastatic breast cancer xenograft, while the DE method cannot (25). When analyzing data, we set $SNR \geq 3$ to eliminate the late-time measurements with poor signal due to T_1 decay. This step is expected to improve the fitting results; a more detailed analysis on the effects of SNR on the accuracy of ratio fitting results can be found in (20).

While the biochemical/biological meaning of lactate labeling signal in HP ¹³C-NMR experiments remains unclear, the kinetic parameters we here reported are a more direct reflection of LDH activity. The significant correlations we found between k_p and the maximum or integrated lactate signal for both control and the 7-day cohort are consistent with what have also been reported in the literature for the LDH-catalyzed reaction (9,26), suggesting that the lactate labeling signal (normalized to pyruvate) might be a good surrogate indicator of the forward rate constant. However, we did see several data points deviating far from the correlation lines (Figure 4). Whether this is due to measurement errors or a possible true violation of the correlation between k_p and the lactate

labeling signal remains to be investigated. We did not find a significant correlation between k_i and the lactate labeling signal for either control or the 7-day cohort, which also needs to be investigated in the future.

This is the first study to quantify the LDH reaction rate constants in perfused rat lungs using HP-NMR and to differentiate between the controls and bleomycin-induced inflamed lungs. It is known that bleomycin pulmonary toxicity is mediated by the immune system with macrophages and lymphocytes being typically found in the lung tissue (27) and may lead to the development of pulmonary fibrosis characterized by enhanced production and deposition of collagen and other matrix components (3). By examining the H&E-stained lung tissue sections, we observed that with one-time bleomycin treatment, rat lungs developed signs of inflammation characterized by higher levels of neutrophils, macrophages, organizing pneumonia foci, and lymphocytes. We observed more macrophages and organizing pneumonia foci at day 21 compared to those at day 7, which probably indicated the inflammation had progressed to a fibrotic state (28). Pulmonary fibrosis is the final phase of many severe lung injuries. Since bleomycin-induced lung injuries are often irreversible without early interventions, we performed HP-NMR measurements on lungs *ex vivo* at two time points (the 7th day and 21st day) post bleomycin treatment in order to understand the progression of lung injury from the perspective of metabolism.

The HP-NMR technique enabled us to correlate the metabolic changes with the histology scores and identify the significant differences in the kinetic parameters between the inflamed lungs observed at the 7-day post-treatment and the control ones. Previously, we found a positive linear correlation between lactate labeling signals and neutrophil count and an approximately three-fold increase in average lactate in the 7-day group compared to controls (19). With new data from 6 additional rats (5 extra in the control and 1 extra in the 7-day group, respectively), the ratiometric fitting analysis yielded consistent results. We see significant positive linear correlations between the rate constants (both k_p and k_i) and the levels of neutrophils (*Figure 3*) and the average k_p had a similar fold of increase (~3.2) at day 7 (*Table 2*). What was not available from our previous analysis (19) is the significant increase of the apparent reverse rate constants k_i of the LDH-catalyzed reaction at day 7. The LDH reaction activity, i.e., the rate of exchange between lactate and pyruvate, is proportional to the apparent first-order rate constants. Thus, the simultaneous increase of

both k_p and k_i suggests higher overall LDH activity, possibly due to increased enzyme concentration. The significant correlations of the rate constants with neutrophil levels (*Figure 3*) suggest that the larger rate constants could be an indicator of lung inflammation.

Another piece of new information we have obtained from this ratiometric analysis is the observation of an increased k_p/k_i ratio between the 7-day and the control groups. Under the near-equilibrium assumption for the LDH reaction, k_p/k_i is proportional to the cellular redox potential NADH/NAD^+ (21,29). Redox potential is a key mediator of many biological processes including metabolism, proliferation, oxidative stress, and signaling (15) and may play important roles in inflammatory disorders (30,31). However, it remains to be investigated whether or not the changes in k_p/k_i as identified in this report reflect a lung redox state modification associated with the injuries (32).

In order to see if and how the kinetic parameters change during lung injury progression, this study also included the analysis on the observations made on day 21 post-treatment. We observed a trend of increased k_p and k_i for the 21-day group with respect to the control, and a trend of increased k_p , decreased k_p and k_p/k_i with respect to the 7-day group, although we did not perform statistical analysis comparing the 21-day group with the other groups due to the low number of lung samples in the 21-day cohort. These late-time trends are likely due to the switch from inflammation to fibrosis (33). It is known that LDH level in the bleomycin-treated rat lung decreases over time and the time of LDH measurement is important for assessing lung damage or inflammation (34-36). Investigation by proton MRI and histology also showed that the rat lung injuries induced by a single administration of bleomycin at 3 mg/kg progressed to fibrotic condition at the 21st day post-treatment (37). Despite the trend of difference between the 7- and 21-day groups, more samples should be investigated regarding the possibility of differentiating early from late stage of lung injuries by the HP-NMR-determined LDH kinetic parameters.

Although the relative changes of the kinetic constants can provide useful information on lung injury, the rate constants of LDH reaction of perfused lung reported in this work are apparent rate constants which may be distorted by the signals from extracellular pyruvate and pyruvate in the perfusate outside the lung. Our work is in process to improve the measurement accuracy of the LDH rate constants by injecting HP ^{13}C -alanine (38) and observing its metabolites pyruvate and the subsequent lactate. We

observed signals of both metabolites in perfused lungs. This approach ensures that the measured pyruvate and lactate signals are mostly intracellular and eliminates the significant contribution from the metabolites in the extracellular space and perfusate.

While aiming for proof-of-concept, this study has some other limitations. Firstly, the experimental model was a perfused lung *ex vivo* rather than the lung in an animal. Secondly, this study did not sample data at time points earlier than 7 days post-treatment, when lung inflammation could have already happened. Thirdly, this study only had three observations in the 21-day group and more should be done in future to acquire injury progression information at more time points. Fourthly, this study did not include a design of varying dosages of bleomycin for inducing lung injuries.

Conclusions

Our ratiometric analysis of HP ^{13}C -NMR lung data provides new information for understanding the metabolic kinetics during lung inflammation. Our results indicate that inflammation changed the apparent forward and reverse rate constants of the LDH-catalyzed reaction and the ratio of the rate constants in the lung tissue. Both rate constants correlated with some histological indices for individual lungs; also the forward rate constant correlated linearly with lactate labeling signal, which may be a surrogate indicator of the forward rate constant despite several data points with large deviations from the correlation.

Acknowledgements

The authors wish to thank Mr. David Nelson for his proof-reading the manuscript.

Funding: This work was funded by United States NIH grant R01-CA155348 (LZ Li) and R01-EB010208 (R Rizi).

Footnote

Conflicts of Interest: The authors have no conflicts of interest to declare.

References

- Ghafoori P, Marks LB, Vujaskovic Z, Kelsey CR. Radiation-induced lung injury. Assessment, management, and prevention. *Oncology (Williston Park)* 2008;22:37-47; discussion 52-3.
- Kawai K, Akaza H. Bleomycin-induced pulmonary toxicity in chemotherapy for testicular cancer. *Expert Opin Drug Saf* 2003;2:587-96.
- Hay J, Shahzeidi S, Laurent G. Mechanisms of bleomycin-induced lung damage. *Arch Toxicol* 1991;65:81-94.
- Albers MJ, Bok R, Chen AP, Cunningham CH, Zierhut ML, Zhang VY, Kohler SJ, Tropp J, Hurd RE, Yen YF, Nelson SJ, Vigneron DB, Kurhanewicz J. Hyperpolarized ^{13}C lactate, pyruvate, and alanine: noninvasive biomarkers for prostate cancer detection and grading. *Cancer Res* 2008;68:8607-15.
- Brindle KM, Bohndiek SE, Gallagher FA, Kettunen MI. Tumor imaging using hyperpolarized ^{13}C magnetic resonance spectroscopy. *Magn Reson Med* 2011;66:505-19.
- Day SE, Kettunen MI, Gallagher FA, Hu DE, Lerche M, Wolber J, Golman K, Ardenkjaer-Larsen JH, Brindle KM. Detecting tumor response to treatment using hyperpolarized ^{13}C magnetic resonance imaging and spectroscopy. *Nat Med* 2007;13:1382-7.
- Kurhanewicz J, Vigneron DB, Brindle K, Chekmenev EY, Comment A, Cunningham CH, Deberardinis RJ, Green GG, Leach MO, Rajan SS, Rizi RR, Ross BD, Warren WS, Malloy CR. Analysis of cancer metabolism by imaging hyperpolarized nuclei: prospects for translation to clinical research. *Neoplasia* 2011;13:81-97.
- Venkatesh HS, Chaumeil MM, Ward CS, Haas-Kogan DA, James CD, Ronen SM. Reduced phosphocholine and hyperpolarized lactate provide magnetic resonance biomarkers of PI3K/Akt/mTOR inhibition in glioblastoma. *Neuro Oncol* 2012;14:315-25.
- Ward CS, Venkatesh HS, Chaumeil MM, Brandes AH, Vancracking M, Dafni H, Sukumar S, Nelson SJ, Vigneron DB, Kurhanewicz J, James CD, Haas-Kogan DA, Ronen SM. Noninvasive detection of target modulation following phosphatidylinositol 3-kinase inhibition using hyperpolarized ^{13}C magnetic resonance spectroscopy. *Cancer Res* 2010;70:1296-305.
- Su JS, Woods SM, Ronen SM. Metabolic consequences of treatment with AKT inhibitor perifosine in breast cancer cells. *NMR Biomed* 2012;25:379-88.
- Lodi A, Woods SM, Ronen SM. Treatment with the MEK inhibitor U0126 induces decreased hyperpolarized pyruvate to lactate conversion in breast, but not prostate, cancer cells. *NMR Biomed* 2013;26:299-306.
- Nelson SJ, Kurhanewicz J, Vigneron DB, Larson PE, Harzstark AL, Ferrone M, van Criekinge M, Chang JW, Bok R, Park I, Reed G, Carvajal L, Small EJ, Munster

- P, Weinberg VK, Ardenkjaer-Larsen JH, Chen AP, Hurd RE, Odegardstuen LI, Robb FJ, Tropp J, Murray JA. Metabolic imaging of patients with prostate cancer using hyperpolarized [1-¹³C]pyruvate. *Sci Transl Med* 2013;5:198ra108.
13. Shaghaghi H, Kadlecek S, Profka H, Siddiqui S, Kuzma N, Ishii M, Rizi RR. The Effect Of Hyperpolarized [1-¹³C] Pyruvate Concentration On Lung Metabolism. *American Thoracic Society International Conference Abstracts: A45. Diagnostic techniques, monitoring and technology. American Thoracic Society; 2013,A1554.*
 14. Kadlecek S, Shaghaghi H, Profka H, Pourfathi M, Siddiqui S, Rizi RR. Hyperpolarized pyruvate signal dynamics in relation to lung redox state. In Copenhagen, Denmark: Proceeding of 4th International DNP Symposium; 2013,39.
 15. Pullinger B, Profka H, Ardenkjaer-Larsen JH, Kuzma NN, Kadlecek S, Rizi RR. Metabolism of hyperpolarized [1-¹³C]pyruvate in the isolated perfused rat lung - an ischemia study. *NMR Biomed* 2012;25:1113-8.
 16. Santyr G, Fox M, Thind K, Hegarty E, Ouriadov A, Jensen M, Scholl TJ, Van Dyk J, Wong E. Anatomical, functional and metabolic imaging of radiation-induced lung injury using hyperpolarized MRI. *NMR Biomed* 2014;27:1515-24.
 17. Thind K, Jensen MD, Hegarty E, Chen AP, Lim H, Martinez-Santesteban F, Van Dyk J, Wong E, Scholl TJ, Santyr GE. Mapping metabolic changes associated with early radiation induced lung injury post conformal radiotherapy using hyperpolarized ¹³C-pyruvate magnetic resonance spectroscopic imaging. *Radiother Oncol* 2014;110:317-22.
 18. MacKenzie JD, Yen YF, Mayer D, Tropp JS, Hurd RE, Spielman DM. Detection of inflammatory arthritis by using hyperpolarized ¹³C-pyruvate with MR imaging and spectroscopy. *Radiology* 2011;259:414-20.
 19. Shaghaghi H, Kadlecek S, Deshpande C, Siddiqui S, Martinez D, Pourfathi M, Hamedani H, Ishii M, Profka H, Rizi R. Metabolic spectroscopy of inflammation in a bleomycin-induced lung injury model using hyperpolarized 1-(¹³C) pyruvate. *NMR Biomed* 2014;27:939-47.
 20. Li LZ, Kadlecek S, Xu HN, Daye D, Pullinger B, Profka H, Chodosh L, Rizi R. Ratiometric analysis in hyperpolarized NMR (I): test of the two-site exchange model and the quantification of reaction rate constants. *NMR Biomed* 2013;26:1308-20.
 21. Li LZ, Xu HN, Kadlecek S, Nath K, Cai K, Hariharan H, Glickson JD, Rizi R. Non-invasive quantification of intracellular redox state in tissue by hyperpolarized ¹³C-NMR. *Proc Intl Soc Mag Reson Med* 2012;20:4308.
 22. Xu HN, Shaghaghi H, Kadlecek S, Profka H, Li LZ, Rizi R. Differentiating injured and normal lungs by the ratiometric analysis of hyperpolarized-¹³C-NMR data. *Proc Intl Soc Mag Reson Med* 2014;22:0773.
 23. Matute-Bello G, Downey G, Moore BB, Groshong SD, Matthay MA, Slutsky AS, Kuebler WM; Acute Lung Injury in Animals Study Group. An official American Thoracic Society workshop report: features and measurements of experimental acute lung injury in animals. *Am J Respir Cell Mol Biol* 2011;44:725-38.
 24. Witney TH, Kettunen MI, Brindle KM. Kinetic modeling of hyperpolarized ¹³C label exchange between pyruvate and lactate in tumor cells. *J Biol Chem* 2011;286:24572-80.
 25. Xu HN, Kadlecek S, Profka H, Glickson JD, Rizi R, Li LZ. Is higher lactate an indicator of tumor metastatic risk? A pilot MRS study using hyperpolarized (¹³C)-pyruvate. *Acad Radiol* 2014;21:223-31.
 26. Bahrami N, Swisher CL, Von Morze C, Vigneron DB, Larson PE. Kinetic and perfusion modeling of hyperpolarized (¹³C) pyruvate and urea in cancer with arbitrary RF flip angles. *Quant Imaging Med Surg* 2014;4:24-32.
 27. O'Sullivan JM, Huddart RA, Norman AR, Nicholls J, Dearnaley DP, Horwich A. Predicting the risk of bleomycin lung toxicity in patients with germ-cell tumours. *Ann Oncol* 2003;14:91-6.
 28. Wynn TA. Integrating mechanisms of pulmonary fibrosis. *J Exp Med* 2011;208:1339-50.
 29. Li LZ, Kadlecek S, Shaghaghi H, Xu HN, Profka H, Rizi R. HP-¹³C-NMR detects the alternation of LDH kinetics and redox state induced by metabolite modulation. *Proc Intl Soc Mag Reson Med* 2014;22:1002.
 30. Rahman I, Adcock IM. Oxidative stress and redox regulation of lung inflammation in COPD. *Eur Respir J* 2006;28:219-42.
 31. Comhair SA, Erzurum SC. Redox control of asthma: molecular mechanisms and therapeutic opportunities. *Antioxid Redox Signal* 2010;12:93-124.
 32. Reddy SP, Hassoun PM, Brower R. Redox imbalance and ventilator-induced lung injury. *Antioxid Redox Signal* 2007;9:2003-12.
 33. Chaudhary NI, Schnapp A, Park JE. Pharmacologic differentiation of inflammation and fibrosis in the rat bleomycin model. *Am J Respir Crit Care Med* 2006;173:769-76.
 34. Drent M, Cobben NA, Henderson RF, Wouters EF, van

- Dieijen-Visser M. Usefulness of lactate dehydrogenase and its isoenzymes as indicators of lung damage or inflammation. *Eur Respir J* 1996;9:1736-42.
35. Chen F, Gong L, Zhang L, Wang H, Qi X, Wu X, Xiao Y, Cai Y, Liu L, Li X, Ren J. Short courses of low dose dexamethasone delay bleomycin-induced lung fibrosis in rats. *Eur J Pharmacol* 2006;536:287-95.
36. Yang MJ, Yang YS, Kim YB, Cho KH, Heo JD, Lee K, Song CW. Noninvasive monitoring of bleomycin-induced lung injury in rats using pulmonary function test. *Toxicological Research* 2008;24:273-80.
37. Babin AL, Cagnet C, Gérard C, Wyss D, Page CP, Beckmann N. Noninvasive assessment of bleomycin-induced lung injury and the effects of short-term glucocorticosteroid treatment in rats using MRI. *J Magn Reson Imaging* 2011;33:603-14.
38. Hu S, Zhu M, Yoshihara HA, Wilson DM, Keshari KR, Shin P, Reed G, von Morze C, Bok R, Larson PE, Kurhanewicz J, Vigneron DB. In vivo measurement of normal rat intracellular pyruvate and lactate levels after injection of hyperpolarized [1-(13)C]alanine. *Magn Reson Imaging* 2011;29:1035-40.

Cite this article as: Xu HN, Kadlecek S, Shaghghi H, Zhao H, Profka H, Pourfathi M, Rizi R, Li LZ. Differentiating inflamed and normal lungs by the apparent reaction rate constants of lactate dehydrogenase probed by hyperpolarized ¹³C labeled pyruvate. *Quant Imaging Med Surg* 2016;6(1):57-66. doi: 10.3978/j.issn.2223-4292.2016.02.04